ICARUS 105, 557–567 (1993)

Water Production Rates in Comet P/Halley from IUE Observations of HI Lyman-α

MICHAEL R. COMBI

Space Physics Research Laboratory, Department of Atmospheric, Oceanic and Space Sciences, University of Michigan, 2455 Hayward Street, Ann Arbor, Michigan 48109-2143
E-mail: combi@sprlc.sprl.umich.edu

AND

PAUL D. FELDMAN

Department of Physics and Astronomy, The Johns Hopkins University, Baltimore, Maryland 21218

Received April 23, 1993; revised August 9, 1993

During the 1985–1986 apparition of Comet P/Halley, the International Ultraviolet Explorer (IUE) satellite observed the comet using both the long-wavelength and short-wavelength spectrographs. The combination of a spherical radiative transfer model and the hybrid gas-dynamic/Monte Carlo model for hydrogen coma, which had been used to analyze H Lyman-α IUE observations of Comet P/Giacobini–Zinner, has been applied to a large body of H observations of Comet Halley taken with the short wavelength spectrograph. The data include nucleus-centered large aperture observations as well as a few serendipitous offset observations. The inferred water production rates from the nucleus-centered observations are compared herein with a self-consistent analysis already performed for the IUE observations of OH. The agreement is quite good despite the high degree of optical depth in the coma during its most active periods. The results imply that, in order to bring the H and OH observations into agreement at all heliocentric distances, a model for OH which accounts for the variation of the outflow speed of the coma with heliocentric distance is required. © 1993 Academic Press, Inc.

I. INTRODUCTION

From the *in situ* results of the various spacecraft flybys of three comets, and modern groundbased and spacecraft based remote sensing, the fact that the atmospheres of most comets are about 80% or more water in the immediate region of the nucleus is well established. Spacecraft results generally confirmed much of what had been inferred about the composition of comets from a century of groundbased observations and 20-plus years of UV, IR, and radio observations (Delsemme 1991). Therefore, the continued observation of water dissociation products, H, OH, and O, is still quite relevant (Feldman 1991). This is especially true since questions regarding the composition of comets as a group, their vaporization rates, evolution, and their role in the Solar System can be answered only by studying many more comets than can ever be visited by future spacecraft.

Recent successes of Monte Carlo simulations of the main water photodissociation products, H and OH, show that it is now possible to make self-consistent analyses of both the abundance and the spatial distributions of these species. The spatial distribution of the H coma has now been modeled for nuclear distances ranging from the inner coma ($\sim 10^4$ km) out to several times 10^7 km. The models are based on the best assessments of the detailed physical processes occurring in the comae of comets—namely photodissociation, molecular collisions, and dusty–gas dynamic flow (Combi and Smyth 1988a,b). The effect of the heliocentric and cometocentric distance dependence of the outflow speed of the coma (Combi 1989) as it pertains to observations of OH has been recently studied (Combi *et al.* 1993) and compared with the standard 1 km sec^{-1} vectorial model (Festou 1981). It was also shown that, for aperture photometric or aperture-integrated spectroscopic data, a vectorial or a Haser model (where the parent lifetime is corrected for the effects of isotropic OH ejection) can be used if the heliocentric distance dependence of the parent outflow speed within the aperture is taken into account.

In 1985 and 1986, Comet Halley became one of the ~50 comets to be observed by the International Ultraviolet Explorer (IUE) satellite. A number of studies have been

[1] Guest Observer with the IUE satellite observatory.

0019-1035/93 $5.00

published regarding important results obtained from those observations (Feldman *et al.* 1987, McFadden *et al.* 1987, Prisant and Jackson 1987). A series of short-wavelength spectra, which includes the emission of hydrogen Lyman-α, was also taken throughout the Halley apparition. A preliminary version of the observed brightnesses was presented by Feldman (1991). Previous difficulties in analyzing these observations have been overcome by using a combination of a hybrid gas-dynamic/Monte Carlo coma model and a spherical raditive transfer model, first applied to observations of Comet P/Giacobini–Zinner (Combi and Feldman 1992, hereafter referred to as paper 1).

The hybrid model was also used to explain the large-scale image of the H coma (Smyth *et al.* 1991), which was constructed from 4 days of line scans by the Pioneer Venus Orbiter Ultraviolet Spectrometer (PVOUVS). Although an analysis of two rocket images of Halley by McCoy *et al.* (1992) used the three-component Maxwellian model of Keller and Meier (1976), they interpreted their parametrized results in terms of the explicit physics included in the Monte Carlo simulations. A preliminary reanalysis of the full 2 months of observations of the H coma by the PVOUVS using the Monte Carlo simulation model, but originally analyzed with a Haser-type model by Stewart (1987), has been reported by Marconi and Smyth (1991). They find that the large discontinuity shown by Weissman (1987) and Feldman (1991) between the last PVOUVS observation on March 5, 1986, and the first postperihelion IUE observation on March 9 may just be due to an artifact of the use of a steady-state model to extract production rates from a large effective aperture over a swath of PVOUVS observations (Stewart 1987).

This paper describes the analysis of the entire set of IUE observations of H Lyman-α that was taken from September 1985 through June 1986. The goals were: (1) to test the combination of the hybrid H coma and spherical radiative transfer models (first applied to the 6 days of observations of comet P/Giacobini–Zinner) on the 28 days of Halley data, in order to compare the inferred water production rates with published OH observations, analyzed alternatively with the standard 1 km sec^{-1} vectorial model and a complementary hybrid model, (2) to test the effectiveness of the radiative transfer model at extremely high optical depths in the Halley data just after perihelion, and finally (3) to compare the model results with the spatially offset observations.

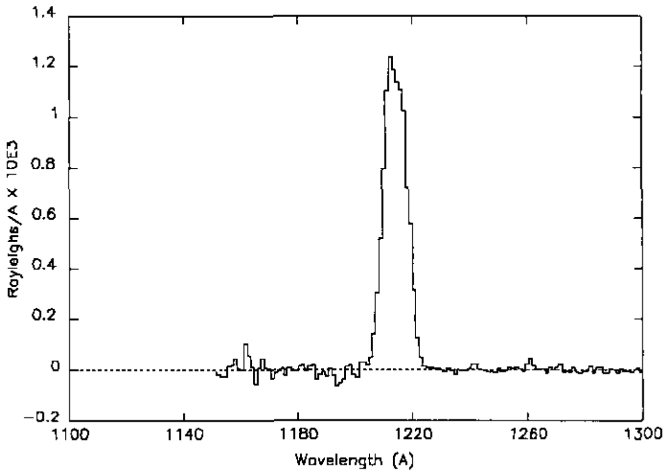

FIG. 1. Spectrum of Comet P/Halley in the H Lyman-α region on December 3, 1985, centered on the nucleus.

II. OBSERVATIONS

The IUE spacecraft, its spectrographs, and the Comet P/Halley observations have already been discussed at length by Feldman *et al.* (1987). The hydrogen Lyman-α emission was recorded in spectra obtained with the short-wavelength primary (SWP) SEC vidicon camera of IUE that covers the spectral range of 1150–1950Å. The measurements of the (0–0) band of OH at ~3090Å in comets were obtained using the long-wavelength primary (LWP) camera. For comet observations the larger entrance aperture (10 × 20 arcsec) is used. The standard calibration and reduction have been discussed in detail by Feldman (1983) and Weaver *et al.* (1981).

Figure 1 shows a sample spectrum of the Lyman-α spectral region on December 3, 1985, with the aperture centered on the nucleus. Table I lists the important observational parameters and the observed Lyman-α brightnesses for each of the observations analyzed for this paper. The contribution to the total signal by geocoronal Lyman-α emission has already been subtracted. For the interpretation of the Halley observations, the subtraction of the geocoronal background turned out to be one of the more difficult problems.

At larger heliocentric distances, the effects of any variation of the outflow speed of the coma have the largest impact on the OH distribution and so represent the most stringent test of the validity of the models and model parameters used. Because of the large ejection speeds of H atoms (8–25 km sec^{-1}) compared with those of the OH radicals (1.05 km sec^{-1}) and the water outflow speed (0.8–1.2 km sec^{-1}), the water production rates determined from H observations should be less dependent on assumptions regarding the outflow speed than those from OH observations. Therefore, the intercomparison of the H and OH observations of Halley at large heliocentric distances might be used to discriminate between various models of the outflow speed. At heliocentric distances near 1 AU the standard 1 km sec^{-1} vectorial model and the hybrid gas-dynamic/Monte Carlo model give essentially the same results.

TABLE I
H Lyman-α Nucleus-Centered Observations of Comet Halley

Date	Spectrum sequence no.	Start time (UT)	Exp. time (sec)	Brightness (Rayleighs)
		Preperihelion 1985		
Sep. 22	SWP26700	1:38:00	3600	1,587
Oct. 20	SWP26958	2:43:13	2700	3,615
Dec. 3	SWP27212	2:29:21	300	12,280
Dec. 16	SWP27287	11:18:55	600	29,260
Dec. 25	SWP27378	2:50:39	120	38,180
Dec. 26	SWP27382	0:35:42	240	35,790
Dec. 29	SWP27409	2:07:23	240	44,140
Dec. 30	SWP27423	16:03:28	90	44,967
Dec. 31	SWP27429	10:53:13	180	55,950
		Postperihelion 1986		
Mar. 9	SWP27885	17:57:02	90	99,467
Mar. 18	SWP27946	23:00:15	90	58,947
Mar. 23	SWP28008	21:14:57	120	46,700
Mar. 25	SWP28014	1:59:00	60	48,540
Mar. 31	SWP28073	23:02:13	120	42,750
Apr. 4	SWP28099	23:45:12	300	39,580
Apr. 10	SWP29135	0:01:00	300	34,730
Apr. 29	SWP28240	20:37:00	600	17,260
May 12	SWP28296	20:45:00	600	12,870
May 16	SWP28317	0:23:08	600	9,980
May 19	SWP28323	20:07:00	600	11,740
May 31	SWP28409	16:47:17	900	6,894
Jun. 8	SWP28458	23:13:26	900	4,361
Jun. 9	SWP28459	4:05:08	1800	4,759
Jun. 12	SWP28478	15:58:29	1800	4,022
Jun. 25	SWP28541	7:17:14	1800	4,654

The observations at relatively larger heliocentric distances were also the faintest observations of the comet, where an uncertainty in the background has the largest effect. For a number of observations the comet was close to the limb of the Earth as seen by IUE, whereas the geocoronal observation was made at some larger distance from the limb. Because of this problem we used a model for the geocorona (McGrath 1992, private communication) which accounts both for the diurnal variation of the hydrogen geocorona and for the path length difference along variously directed lines of sight. In this way a measurement of the geocoronal background taken in a different direction and time from the comet could be extrapolated to the comet's location and time. The set of geocoronal observations is given in Table II. For the observations from mid-December 1985 through mid-April 1986 the comet was much brighter than the background so no separate background was taken, and a 1 kilorayleigh value was assumed.

Extrapolations of geocoronal observations to times of comet observations several days away, using the daily averages of the solar Lyman-α flux measured by the Solar Mesosphere Explorer (SME) satellite, proved to be a very unreliable process for some of the days in the late postperihelion period. In some instances the process yielded geocoronal extrapolations that were larger than the actual comet + background measurements. Such extrapolations yielded wildly varying results, so we concluded the process appeared to be totally unreliable. For this reason we were forced to drop several days of observations from our analysis. The June 25 observation of the comet was made just off the limb of the Earth as seen from IUE, and, although there was a geocoronal measurement taken less than 2 hr later, the extrapolation was very unreliable. Fortunately, 21 of the 28 observations could be used. These included the earliest observation in September 1985 which had the lowest production rate expected from the previously published OH analyses, in addition to some spatially offset observations.

The small and large IUE apertures are offset by 66.3 arcsec in the focal plane of IUE. Since an SWP spectrum can be recorded any time an LWP observation is made, the SWP will see a region of the coma offset by this amount in a known direction from the nucleus. In paper 1

TABLE II
H Lyman-α Geocorona Background Observations

Date	Spectrum	Start time (UT)	Exp. time (sec)	Brightness (Rayleighs)
Sep. 22	SWP26701	3:33:00	3600	772.8
Oct. 20	SWP27959	4:05:00	2700	980.0
Dec. 2	SWP27206	9:54:35	600	4123
Dec. 3	SWP27213	4:20:49	1200	1256
Mar. 23	SWP28009	22:50:36	120	2368
May 19	SWP28344	22:08:00	900	1052
Jun. 25	SWP28542	8:40:49	1800	2114

we made use of a number of "serendipity" and purposeful offset observations of Comet P/Giacobini–Zinner to compare the variation of the Lyman-α brightness in the coma with that determined by the model which reproduced the nucleus-centered observation. The results of that paper indicated that the model accurately reflected the spatial distribution from within the nucleus-centered aperture covering distances smaller than 2500 km out to offset measurements from 7500 to 41,000 km. The H model had been used before to reproduce the very wide field rocket and spacecraft images covering distances out to several times 10^7 km. Although the velocity distribution which shapes the outer coma through radiation pressure and orbital mechanics depends upon modeling the physics taking place in the inner coma, this was the first successful attempt to compare the model with data at these close distances to the nucleus. Table III provides a list of relevant parameters regarding the offset observations.

III. WATER PRODUCTION RATES FROM H LYMAN-α

The procedure for extracting production rates from the Lyman-α brightnesses was described in paper 1. The H coma model used for comet Halley with its implicit time dependence has been described in detail in previous papers. The various strengths and weaknesses of the assumptions have been discussed at length both in paper 1 and in the paper on the reanalysis of the IUE OH observations (Combi *et al.* 1993). For the sake of completeness a brief summary of the model and various parameters follows. The comet Halley H model in particular was described by Smyth *et al.* (1991) in the analysis of the PVOUVS image of 2–6 February 1986. The time variation of inner coma conditions was taken from the results of Combi (1989) which explained Doppler and other velocity-resolved observations of the comet at various heliocentric distances. The water lifetime was taken as 8.2×10^4 sec at 1 AU, and the heliocentric-velocity-dependent OH lifetime was taken from the combined results of Schleicher and A'Hearn (1988) for the near UV photodissociation component and van Dishoeck and Dalgarno (1984) for the Lyman-α component. The dissociation of water has recently been completely reviewed by Budzien (1992), and this value is found to be quite appropriate for Halley and G–Z in the quiet-Sun conditions of 1985 and 1986. The revised picture for water photodissociation and the excess energy for fragments from the results of Crovisier (1989) have been used.

The model includes an implicitly assumed secular variation of production rate with time. This affects the calculated production rates only in indirect and largely second-order ways. The assumed long-term time dependence varies slowly compared with the residence times of H atoms within the relatively small region sampled by the IUE aperture, even for the offset observations, and so has only limited effect on the production rate deduced. Similarly for observations made during times of the 7-day periodic variation of the comet (Schleicher *et al.* 1990), strongest in March and April of 1986, the filling time of the IUE observation is still rather short so the inferred production

TABLE III
H Lyman-α Offset Observations of Comet Halley

Date	Spectrum	Offset (arcsec)	Start (UT)	Exp. (sec)	Total (Rayleighs)
Oct. 20	SWP26957	66.3	0:40:26	3600	892
Dec. 2	SWP27207	42.6	11:39:32	600	6567
May 16	SWP28318	66.3	1:19:26	1500	2371

rate will represent an average value having a small phase lag (a few hours) and compression (~10%) of the true amplitude of the variation of the actual gas production rate at the nucleus (Combi and Fink 1993).

As in paper 1, the H coma model was run for each nucleus-centered observation. This yields a normalized H atom density profile as a function of distance from the nucleus, which, when multiplied by a water production rate, produces a radial density profile (in cm^{-3} for example). The spherical radiative transfer model was then run for each of three values of the instantaneous water production rate: one at that estimated from the nearest (in time) gas-dynamic/Monte Carlo model applied to the OH observation (Combi *et al.* 1993), and two others each 30% higher and lower than that value. This yields predicted Lyman-α brightnesses for three values of the water production rate. The best production rate is found by a logarithmic interpolation using those three values, since the optical thickness causes the transfer function from brightness to production rate to be highly nonlinear, especially when the production rates were large in the 3 months surrounding perihelion.

The radiative transfer model, adapted from the method of Anderson and Hord (1977), is run in two steps. The first step calculates the radiation field in an axisymmetric region around the coma running from 10^2 to 10^7 km in radius from the nucleus and in 16 angular sectors. The second step integrates lines-of-sight on a desired grid of values given the Sun–comet–observer angle and solar flux at the heliocentric Doppler shift of the comet. The model produces a 20 × 40 grid which is set to be large enough so that is just overfills the IUE aperture. The average brightness within the modeled aperture is then calculated in a last step by integrating over the gridded values within the projected aperture.

The H coma model also accumulates the appropriate kinetic information to provide an effective measure of the "temperature" that is required for the radiative transfer calculation. This is not a temperature in the literal sense but simply a single parameter that describes the average width of the velocity distribution of H atoms in the coma owing to the effects of all components: photodissociation ejection, partial thermalization, and outflow speed. The definition in kinetic terms was given in paper 1. The temperatures found for all comet models run both in paper 1 for comet P/Giacobini–Zinner and for these in Halley are within a few hundred degrees of 14,000 K. This is in fact what one would expect from a distribution dominated by the major 8 and 18 km sec^{-1} components from OH and H_2O photodissociation which are spread out and randomized by collisions and addition of the outflow component. In cases where a large fraction of H atoms would be thermalized (i.e., at very small heliocentric distances, ≤0.5 AU, and large production rates) a more complicated scheme might be required, especially if the velocity distribution is not isotropic. In this case, 14,000 K would be inappropriate, and a somewhat smaller temperature could work reasonably well. For Halley only a few percent of H atoms are completely thermalized (McCoy *et al.* 1992), and the 14,000 K "temperature" does in fact represent the speed distribution of H atoms quite well, as shown in paper 1.

The resonance scattering rate of the solar Lyman-α emission by H atoms depends of course directly on the solar flux at the Doppler shift of the atoms. As in paper 1, we adopted the solar Lyman-α flux from the day-to-day measurements by SME and the shape of the solar line profile from Lemaire *et al.* (1978). However, in paper 1 we noted a 15% systematic difference between the water production rates calculated using the H and OH observations. The most recently updated version of the SME database (Rottman 1993, private communication) claims a 15% overall calibration uncertainty in their quoted Lyman-α fluxes but a much better relative time-dependent uncertainty, which is no worse than 1–2% per year due to detector degradation. The SUSIM (Solar Ultraviolet Spectral Irradiance Monitor) experiment has been flown twice on the Space Shuttle Spacelab-2 mission, in August 1985, which was during the Halley/Giacobini–Zinner observation period, and again last year (van Hoosier *et al.* 1988). The SUSIM experiment was designed specifically for accurate absolute calibration and claims a much better 5% photometric error.

The solar Lyman-α flux on August 4, 1985, was measured by both instruments. The SUSIM value was 3.24×10^{11} photons cm^{-2} sec^{-1} $Å^{-1}$ or 16% higher than the SME value for that day which was 2.79×10^{11} photons cm^{-2} sec^{-1} $Å^{-1}$. We have renormalized the day-to-day variation of the SME fluxes by this ratio. With this correction, production rates determined from the Lyman-α observations of comets would decrease by 16%. This removes the ~15% systematic difference between the OH- and Lyman-α-determined production rates given in paper 1 for Comet P/Giacobini–Zinner. In that paper we described that calibration uncertainties were typically on the order of 15%. Differences which are on the order of the expected error are nonetheless troublesome. In this paper we use the higher renormalized SME values for computation of water production rates. It is most interesting to note that if we use the original SME fluxes alone the average of the point-by-point ratios of the water production in Halley determined from H are on the average 14% higher than those determined from OH, which is nearly exactly the same as the 15% found in paper 1 for Comet P/Giacobini–Zinner and as the 16% difference between SME and SUSIM.

Table IV lists the water production rates determined from the 21 days of IUE Lyman-α observations when an

TABLE IV
Water Production Rates in Comet Halley from IUE Observations of OH and H

Date (1985–1986)	r (AU)	Δ (AU)	B(Ly-α) (Rayleigh)	β (deg)	F (photons cm^{-2} sec^{-1})	log $Q_{OH}(H_2O)$ (sec^{-1})	log $Q_H(H_2O)$ (sec^{-1})
				Preperihelion 1985			
Sep. 22	2.46	2.33	1,587	23.8	4.81×10^{10}	28.400	28.429
Oct. 20	2.09	1.43	3,615	25.0	7.24×10^{10}	28.743	29.016
Dec. 3	1.45	0.65	12,280	34.0	1.37×10^{11}	28.987	28.978
Dec. 16	1.25	0.84	29,260	51.6	2.09×10^{11}		29.143
Dec. 25	1.13	1.00	38,180	54.6	2.29×10^{11}	29.582	29.509
Dec. 26	1.11	1.02	35,790	54.7	2.47×10^{11}	29.348	29.338
Dec. 29	1.05	1.10	44,140	54.3	2.81×10^{11}	29.476	29.375
Dec. 30	1.03	1.14	44,967	53.8	2.93×10^{11}	29.572	29.331
Dec. 31	1.02	1.16	55,950	53.4	3.15×10^{11}	29.555	29.452
Mar. 9	0.84	1.06	99,467	61.6	4.49×10^{11}	29.818	29.734
Mar. 18	0.98	0.84	58,947	66.1	2.86×10^{11}	29.642	29.691
Mar. 23	1.04	0.73	46,700	66.2	2.55×10^{11}	29.382	29.263
Mar. 25	1.07	0.69	48,540	65.0	2.40×10^{11}	29.728	29.663
Mar. 31	1.18	0.53	42,750	57.5	2.16×10^{11}	29.649	29.483
Apr. 4	1.24	0.46	39,580	49.1	1.92×10^{11}	29.332	29.526
Apr. 10	1.32	0.42	34,730	34.8	1.64×10^{11}	29.367	29.343
Apr. 29	1.62	0.77	17,260	28.4	1.03×10^{11}	29.134	29.424
May 12	1.81	1.18	12,870	31.5	8.64×10^{10}	29.334	29.500
May 16	1.85	1.28	9,980	31.4	8.27×10^{10}	29.340	29.406

Note. r, heliocentric distance; Δ, geocentric distance; β, Sun–comet–Earth angle; F, solar Lyman-α flux at the comet's heliocentric distance and velocity; B, observed cometary Lymman-α brightness in Rayleighs; $Q_{OH}(H_2O)$, water production rate from H Lyman-α observation; $Q_H(H_2O)$, water production rate from OH observation.

adequate estimate of the geocorona background could be made. We have compared these with the water production rates determined from the IUE OH observations using both the comparable hybrid gas-dynamic/Monte Carlo analysis and the standard 1 km sec^{-1} vectorial model (Combi *et al.* 1993). We find that, although there is some scatter in the comparison, the hybrid model results for OH provide a better overall match than do the standard constant 1 km sec^{-1} vectorial model. The scatter is indicative of (actually somewhat smaller than) the expected uncertainties estimated from the background subtraction and the calibration between the LWP and SWP convolved through the nonlinear radiative transfer function. The results are plotted in Fig. 2. The agreement between H and OH measurements is quite good on the average ranging from lowest production rate at the largest preperihelion heliocentric distance observations on September 22, 1985, to the highest production rate a month after perihelion on March 9, 1986.

The most stringent comparison is the observation of September 22 where the 61% difference between the water production rates determined from the OH observations using a 1 km sec^{-1} vectorial model and that using the hybrid gas-dynamic/Monte Carlo model was the largest. This is larger than any calibration or model-induced uncertainty. The fact that the hybrid models for both H and OH agree, but that the hybrid H model does not agree with the OH vectorial model, is significant. The results of Combi *et al.* (1993) clearly show that the 1 km sec^{-1} vectorial and hybrid models give essentially the same results near 1 AU but diverge away from 1 AU. However, the H coma at larger heliocentric distances is far less

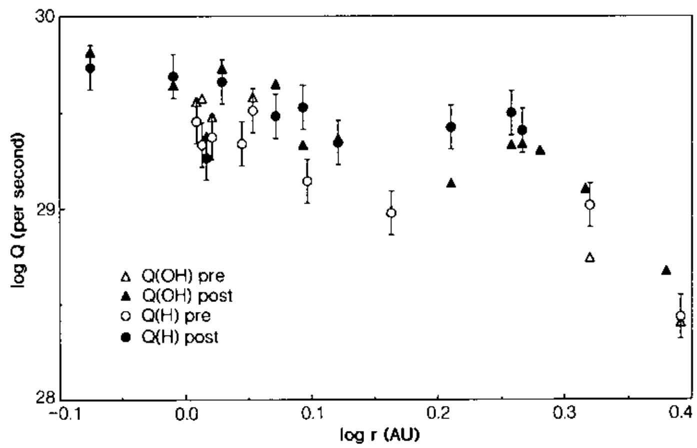

FIG. 2. Comparison of water production rates in Comet P/Halley determined from the IUE observations H Lyman-α with those determined by Combi *et al.* (1993) from the OH observations at 3090 Å and a self-consistent hybrid gas-dynamic/Monte Carlo model analysis.

sensitive to the assumptions regarding the parent outflow speed than is OH.

To validate this point we have generated an H coma model with a parent outflow speed of 1 km sec^{-1}. It is then directly analogous to the 1 km sec^{-1} vectorial model analysis of the September OH observation that yields a water production rate 61% higher than the hybrid gas-dynamic/Monte Carlo model. For the September 22 conditions the production rates were quite low (a few $\times 10^{28}$ per second with either model) and the photochemical lifetimes for all species were long (6 times larger than at 1 AU) because of the large heliocentric distances (2.46 AU). Collisions therefore played almost no role in the H coma. Because of this and the fact that the H atom speeds are much larger than the outflow speed, there is virtually no difference between the H atom 1 km sec^{-1} model and the H atom hybrid model—for September 22, that is. As expected, the H models yield the same production rates to within ~2% (±4%, 3σ) with the H atom vectorial model implying a *slightly smaller* production rate—the OH vectorial model yields a production rate that is *61% larger!* For observations closer to 1 AU all models give the same results. Therefore, we conclude that the preferred agreement between production rates extracted from the H coma model, which is insensitive to the water outflow speed at large heliocentric distances, and the hybrid model analysis of the OH observations implies that the magnitude of the decrease of outflow speed with increasing heliocentric distance is correct.

IV. SPATIAL DISTRIBUTION OF HYDROGEN

On September 21, October 20, November 5, 1985, and May 16, 1986, several SWP observations were made at displacements of 66.3 arcsec from the nucleus. On December 2, 1985, a 42.6-arcsec offset observation was made. The September flux from the comet was just too close to the geocoronal background value to provide any useful information. The nucleus-centered observation on November 4 (a few hours before the November 5 offset) was saturated, so there is no standard with which to compare the offset value. This left three useful measurements. The combination of the H coma and radiative transfer models produces a full description of the brightness field so these offset observations were used to test the spatial variation in the model. Using the best-fit nucleus-centered models for these dates the various offset brightnesses were calculated and are compared with the observed brightnesses in Table V.

Figure 3 shows the layout of the IUE large apertures in both the short- and the long-wavelength cameras during both nucleus-centered SWLA and serendipity SWLA offset observations. These serendipity offsets are actually recorded with the large aperture centered on the nucleus.

TABLE V
Spatial Offset Observations of H Lyman-α of Comet Halley

Date (1985–1986)	Offset (arcsec)	Observed brightness (Rayleighs)	Model brightness[a] (Rayleighs)
Oct. 20	66.3″	892 ± 380	947
Dec. 2	42.6″	6567 ± 2200	4646
May 16	66.3″	2371 ± 1013	3210

[a] Model brightnesses were derived from the models of the nucleus-centered observations in Table IV). Uncertainties account for an approximate uncertainty of 15% per measurement.

The contour plot of surface brightness in the figure corresponds to the model scaled to the nucleus-centered brightness. Although there were no multiple offset observations in different directions on a single day, enabling a measure of optical-depth-induced asymmetry, the conditions on October 20 were such that the coma was largely optically thin. In this case, the model clearly shows that the brightness distributions of the coma should be quite circular.

One problem with all of the Halley offset measurements is that they were taken when the comet's water production rate was small, and the offset surface brightnesses were comparable to or actually smaller than the extrapolated geocoronal background measurements. The resulting background-subtracted surface brightness of the comet has a rather large uncertainty. While not making the measurement totally meaningless, the comparison is not as conclusive as were the results for Comet P/Giacobini–Zinner in paper 1. In that case there were a number of contributing factors helping the offset measurements: there were offsets as small as 22 arcsec, the comet was closer to the Earth, the comet was brighter (in August 1985), and/or the geocorona values were small because the view was farther from the Earth's limb. Because of this, whereas the offsets for Halley generally agree with the modeled value predicted from the nucleus-centered observations, the uncertainties are rather large so the "agreement" is less compelling than in the case for Giacobini–Zinner in paper 1.

The radiative transfer model implies a small asphericity along the comet–Sun line as projected on the sky plane which results from a shadow effect on the antisunward side when the water production rate is large. Since for the Comet Halley observations this asymmetry was only predicted to be a few percent, and since it is clear that the "scatter" is generally larger than this, we present in the table only radially averaged model values. It is possible that in future work such asphericity will prove useful and will be investigated, however, for now we consider it to be at the noise level. It would be very interesting to make Lyman-α images of comparable quality and spatial

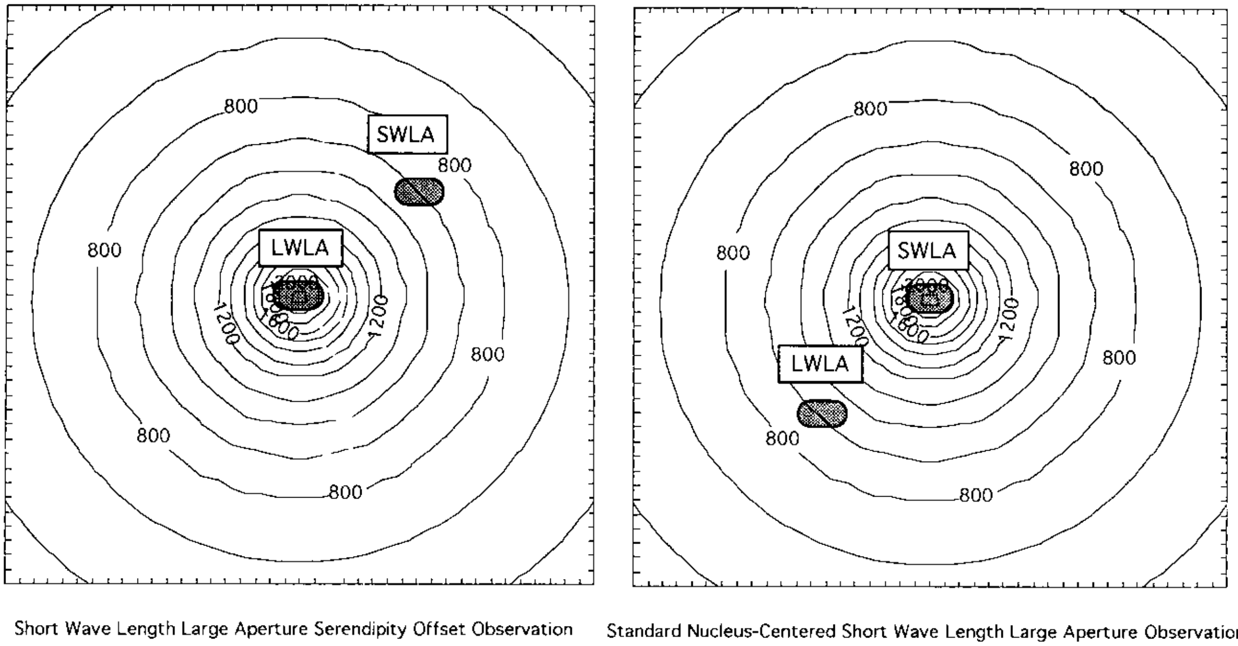

FIG. 3. Geometry for SWLA nucleus-centered and serendipity offset observations for Comet P/Halley on October 20, 1985. (Right) The standard nucleus-centered short-wavelength large aperture (SWLA) observation with the position of long-wavelength aperture (LWLA) shown. When a LWLA spectrum is taken a simultaneous "serendipity" SWSA spectrum can also be taken with the given offset of 66.3 arcsec. The contour plot corresponds to the modeled Lyman-α surface brightness in Rayleighs. The nucleus-centered brightness was 3615 Rayleighs and the offset brightness was 980 Rayleighs. The model is scaled to the nucleus-centered value so that an offset model value of 892 Rayleighs results. This, however, is well within the expected uncertainties.

resolution to that obtained with groundbased telescopes using visible range filtered CCD imaging and compare the small shadow effect with the radiative transfer model.

V. DISCUSSION

Although we find good agreement between the water production rates found from self-consistent observation and analysis of H and OH, there are nonetheless a number of obvious sources of potential error: (1) the H Lyman-α g-factor as derived from the SUSIM/SME solar fluxes and the Lemaire *et al.* (1978) quiet-Sun solar line profile, (2) the OH g-factors taken from Schleicher and A'Hearn (1988), (3) the internal calibration difference between the SWP and LWP cameras within IUE, and (4) errors in the model lifetimes and branching ratios. Individually, these errors could yield discrepancies between H and OH water production rates in the range of 5 to 15%.

The variation of outflow speed with heliocentric distance has some important consequences in the analysis of many kinds of observations of comets, but especially those at large heliocentric distance. Although the use of Haser's model and its radial scale lengths for the calculation of production rates of various species can be done properly, the heliocentric-distance dependence of the parent outflow speed has an implied dependence for the parent scale length. This is in addition to the explicit component of the parent outflow speed, the Q/v term, to which the entire spatial distribution is proportional. Determinations of Haser model scale lengths are complicated by two main factors, namely the relative insensitivity and ambiguity of spatial profile shapes to variation in the Haser model scale lengths and the time variation of gas production rates. Despite this, it does appear, at least for the cases of NH_2 and CN, that the spatial profiles are consistent with photochemical production by a parent species having a Haser parent scale length that varies by less than heliocentric distance squared (Combi and Delsemme 1986, Fink *et al.* 1991). Values in the range of $r^{1.5}$ to $r^{1.8}$ seem to be the best.

Since different species are produced at different ranges of distance from the nucleus and since the outflow speed of the coma also varies with distance from the nucleus, different species should show different parent outflow speeds in the same comet at the same time. For instance, NH_3, the likely source of NH_2, has a short lifetime (~8000 sec at 1 AU), the CN parent has a lifetime in the range of a few $\times\ 10^4$ seconds, and water, which produces OH, has a lifetime of ~80,000 sec. The region from a few thousands to a few tens of thousands of kilometers coincides with the main region of "acceleration" of the outflow due to photochemical heating for a productive comet in the vicinity of 1 AU from the Sun (Lämmerzahl *et al.* 1986, Bockelée-Morvan and Crovisier 1987, Combi 1989, Bockelée-Morvan *et al.* 1990). Therefore, the outflow speed where NH_2 is produced will be several tenths of a kilometer per second less than that where OH is produced. As shown by Combi *et al.* (1993), the situation could be complicated even by the spatial scale of the observation itself, where effective parent molecule outflow speeds for different heliocentric distances were suggested. This enabled a vectorial model to reproduce the same water production rate as the full hybrid model calculation. This is important to understand, especially when using either a vectorial or Haser model and employing an assumed variation of the parent molecule outflow speed with heliocentric distance.

Finally, we have restricted the comparison of our production rates in Comet P/Halley determined from H Lyman-α to those determined from the IUE observations of OH only, for a number of reasons. Various water production rates determined in the optical and UV, including the OH IUE results, have already been summarized by Combi *et al.* (1993). The comparisons of production rates determined from radio observations of OH with those measured by IUE, including the questions regarding collisional quenching and other difficulties in resolving radio and UV observations of OH, have been discussed at length in the recent review by Crovisier and Schloerb (1991) as well as in original papers by Bockelée-Morvan *et al.* (1987), Schloerb *et al.* (1987), Schloerb (1988), and Tacconi-Garman (1989). There were a few direct IR observations of water, both on Vega (Moroz *et al.* 1987) and airborne (Weaver *et al.* 1987, Larson *et al.* 1986), showing general confirmation of the level of the water production rates inferred from the OH UV observations. We chose to leave out groundbased OH observations, since they are typically analyzed using Haser's model. This, depending upon the choice of scale lengths, introduces systematic differences on the order of a factor of 2 with the vectorial model results (Weaver *et al.* 1981). Careful comparisons seem to indicate that there is resonable agreement (Schleicher *et al.* 1987). Last, the main reason for restricting this comparison between H and OH observations with IUE is that it enables us to make self-consistent comparisons of data taken with the same instrument at nearly the same time, and, most importantly, analyzed with self-consistent model assumptions.

Now that we have a demonstrated self-consistent approach to analyzing simultaneous H and OH in comets as observed by IUE, there are a number of important studies that can be made. The set of about 50 comets observed by IUE spans more than one complete solar cycle. Simultaneous H and OH observations should be sensitive to two important parameters that are believed to vary markedly with solar activity. These are the shape of the solar Lyman-α line profile and the dissociation rate of water and to a lesser extent of OH.

Oppenheimer and Downey (1980) also noted the importance of the variation of solar Lyman-α to the dissociation of water and concluded that the overall rate could vary by up to a factor of two with solar activity. In addition, the ratios between the ionization, the H + OH, the H_2 + $O(^1D)$, and the 2H + O dissociation branches should also vary with solar activity. Because of this the water lifetime used in the reduction of both the OH observations and the H observations should also vary over the solar cycle. We can test this variation by comparing the observations and resultant water production rates between solar minimum and solar maximum and varying or not varying the lifetimes in the model. It is not clear to what extent the relative H and OH abundances as seen by IUE near the nucleus are affected by varying the water lifetime. It is clear that the absolute abundances of each should be affected.

The other interesting question, which could be investigated by the self-consistent analysis of H and OH, is the variation of the shape of the solar Lyman-α profile with solar activity over the 11-year cycle. In our large-scale coma modeling and in the radiative transfer calculations we have used the average quiet-Sun full-disk H Lyman-α profile shape determined by Lemaire *et al.* (1978). However, recent work by Fontenla *et al.* (1988), who observed the Lyman-α profile in local regions of the Sun during various levels of activity, found that the shape of the profile within those regions changed dramatically. No one yet knows, however, how the full-disk-averaged value changes with solar activity.

The agreement of the water production rates determined from OH and H observations, when using self-consistent models that account for the correct dependence of the outflow speed on heliocentric distance, has important consequences for the heliocentric-distance dependence of gas production rates that are deduced from observations. As discussed already by Combi *et al.* (1993), the inclusion of the variation of outflow speed results in production rates that are smaller at large heliocentric distances and larger at smaller heliocentric distances. This has the effect of increasing the magnitude of the exponent in the heliocentric distance law (r^{-n}) by about 0.5. Even more important corrections should be expected for gas production rates calculated at very large heliocentric distances such as for CN in P/Halley at 4.7 AU (Wyckoff *et al.* 1985) or even in objects such as Chiron at 11.3 AU (Bus *et al.* 1991).

ACKNOWLEDGMENTS

We thank Mr. Scott Cochran who helped process some of the model analysis as part of the Research Experience for Undergraduates program funded by the NSF. We thank again J. Bishop for providing us with a cometary coma version of his radiative transfer code and for help in implementing it. We thank M. McGrath for providing with the geocorona model, E. Roettger for help with accessing the IUE comet data base at Johns Hopkins, and G. Rottman, D. Schleicher, and M. van Hoosier for useful conversations. We also thank two anonymous referees for careful reading and helpful suggestions. Support for this work came from the NASA Astrophysics Data Program in the form of Grant NAG 5-1333 to University of Michigan. The work at J.H.U. was supported by NASA Grants NSG-5393 and NAG-5-2141.

REFERENCES

ANDERSON D. E. JR., AND C. W. HORD 1977. Multidimensional radiative transfer: Applications to planetary coronae. *Plan. Space Sci.* **25,** 563–571.

BOCKELÉE-MORVAN, D., AND J. CROVISIER 1987. The role of water in the thermal balance of the coma. In *Proceedings of the Symposium on the Diversity and Similarity of Comets.* ESA SP 277, pp. 235–240.

BOCKELÉE-MORVAN, D., J. CROVISIER, D. DESPOIS, T. FORVEILLE, E. GERARD, J. SCHRAML, AND C. THUM 1987. Molecular observations of comets P/Giacobini–Zinner 1984e and P/Halley 1982i at millimetre wavelengths. *Astron. Astrophys.* **180,** 253–262.

BOCKELÉE-MORVAN, D., J. CROVISIER, AND E. GERARD 1990. Retrieving the coma gas expansion velocity in P/Halley, Wilson (1987 VII) and several other comets from the 18-cm OH line shapes. *Astron. Astrophys.* **238,** 382–400.

BUDZIEN, S. A. 1992. Ph.D. thesis, Johns Hopkins University.

BUS, S. J., M. F. A'HEARN, D. G. SCHLEICHER, AND E. BOWELL 1991. Detection of CN emission from (2060) Chiron. *Science* **251,** 774–777.

COMBI, M. R. 1989. The outflow speed of the coma of Halley's comet. *Icarus* **81,** 41–50.

COMBI, M. R., B. J. BOS, AND W. H. SMYTH 1993. The OH distribution in cometary atmospheres: A collisional Monte Carlo model for heavy species. *Astrophys. J.* **408,** 668–677.

COMBI, M. R., AND A. H. DELSEMME 1986. Neutral Cometary Atmospheres. V. C_2 and CN in Comets. *Astrophys. J.* **308,** 472–484.

COMBI, M. R., AND P. D. FELDMAN. 1992. IUE observations of HI Lyman-α in comet P/Giacobini–Zinner. *Icarus* **97,** 260–268.

COMBI, M. R., AND U. FINK. 1993. P/Halley: Effects of time-dependent production rates on spatial emission profiles. *Astrophys. J.* **409,** 790–797.

COMBI, M. R., AND W. H. SMYTH. 1988a. Monte Carlo particle trajectory models for neutral cometary gases. I. Models and equations. *Astrophys. J.* **327,** 1026–1043.

COMBI, M. R., AND W. H. SMYTH. 1988b. Monte Carlo particle trajectory models for neutral cometary gases. II. The spatial morphology of the Lyman-alpha coma. *Astrophys. J.* **327,** 1044–1059.

CROVISIER, J. 1989. The photodissociation of water in cometary atmospheres. *Astron. Astrophys.* **213,** 459–464.

CROVISIER, J., AND F. P. SCHLOERB. 1991. The study of comets at radio wavelengths. In *Comets in the Post-Halley Era* (R. L. Newburn, Jr., *et al.*, eds.), Vol. 1, pp. 149–173. Kluwer Academic, The Netherlands.

DELSEMME, A. H. 1991. Nature and history of the organic compounds in comets: An astrophysical view. In *Comets in the Post-Halley Era* (R. L. Newburn, Jr., *et al.*, eds.), Vol. 1, pp. 377–428. Kluwer Academic, Netherlands.

FELDMAN, P. D. 1983. Ultraviolet spectroscopy and the composition of cometary ice. *Science* **219,** 347–354.

FELDMAN, P. D. 1991. Ultraviolet spectroscopy of cometary comae. In *Comets in the Post-Halley Era* (R. L. Newburn, Jr., *et al.* eds.), Vol. 1, pp. 139–148. Kluwer Academic, The Netherlands.

FELDMAN, P. D., *et al.* 1987. IUE observations of comet P/Halley: Evolution of the ultraviolet spectrum between September 1985 and July 1986. *Astron. Astrophys.* **187,** 325–328.

FESTOU, M. C. 1981. The density distributions of neutral compounds in cometary atmospheres. II. Production rate and lifetime of OH radicals in comet Kobayashi–Berger–Milon (1975 IV). *Astron. Astrophys.* **96,** 52–57.

FINK, UWE, MICHAEL R. COMBI, AND MICHAEL A. DISANTI 1991. P/Halley: Spatial distributions and scale lengths for C_2, CN, NH_2 and H_2O. *Astrophys. J.* **383,** 356–371.

FONTENLA, J., E. J. REICHMANN, AND E. TANDBERG-HANSSEN 1988. The Lyman-alpha line in various solar features. I. Observations. *Astrophys. J.* **329,** 464–481.

KELLER, H. U., AND R. R. MEIER 1976. A cometary hydrogen model for arbitrary observational geometry. *Astron. Astrophys.* **52,** 273–281.

LÄMMERZAHL, P., *et al.* 1986. Expansion velocity and temperature of gas and ions measured in the coma of comet Halley. In *Exploration of Halley's Comet*, pp. 179–182. ESA SP-320.

LARSON, H. P., M. J. MUMMA, H. A. WEAVER, AND D. S. DAVIS 1986. Velocity-resolved observations of water in comet Halley. *Astrophys. J. Lett.* **309,** L95–L99.

LEAN, J. 1987. Solar ultraviolet irradiance variations: A review. *J. Geophys. Res.* **92,** 839.

LEMAIRE, P., J. CHARRA, A. JOUCHOUX, A. VIDAL-MADJAR, G. ARTZNER, J. C. VIAL, R. M. BONNET, AND A. SKUMANICH 1978. Calibrated full disk solar HI Lyman-alpha and Lyman-beta profiles. *Astrophys. J.* **223,** L55–L58.

MARCONI, M. L., AND W. H. SMYTH 1991. The production of H_2O by Halley close to perihelion. *Bull. Am. Astron. Soc.* **23,** 1168.

MCCOY, R. P., R. R. MEIER, H. U. KELLER, AND G. R. CARRUTHERS 1992. The hydrogen coma of comet P/Halley observed in Lyman α using sounding rockets. *Astron. Astrophys.* **258,** 555–565.

MCFADDEN, L. A., M. F. A'HEARN, P. D. FELDMAN, E. E. ROETTGER, D. M. EDSALL, AND P. S. BUTTERWORTH 1987. Activity of comet P/Halley 23–25 March, 1986. IUE observations. *Astron. Astrophys.* **187,** 333–338.

MOROZ, V. I., *et al.* 1987. Detection of parent molecules in comet P/Halley from the IKS-Vega experiment. *Astron. Astrophys.* **187,** 513–518.

OPPENHEIMER, M., AND C. J. DOWNEY 1980. The effect of solar-cycle ultraviolet flux variation on cometary gas. *Astrophys. J.* (*Lett.*) **241,** L123–L127.

PRISANT, M. G., AND W. M. JACKSON 1987. A rotational-state population analysis of the high-resolution IUE observations of CS emission in comet P/Halley. *Astron. Astrophys.* **187,** 489–496.

SCHLEICHER, D. G., AND M. F. A'HEARN 1988. The fluorescence of cometary OH. *Astrophys. J.* **331,** 1058–1077.

SCHLEICHER, D. G., R. L. MILLIS, AND P. V. BIRCH 1987. Photometric observations of comet P/Giacobini–Zinner. *Astron. Astrophys.* **187,** 531–538.

SCHLEICHER, D. G., R. L. MILLIS, D. T. THOMPSON, P. V. BIRCH, R. M. MARTIN, D. J. THOLEN, J. R. PISCITELLI, N. L. LARK, AND H. B. HAMMEL 1990. Periodic variations in the activity of comet P/Halley during the 1985/1986 apparition. *Astron. J.* **100,** 896–912.

SCHLOERB, F. P. 1988. Collisional quenching of cometary emission in the 18 centimeter OH transitions. *Astrophys. J.* **332,** 524–530.

SCHLOERB, F. P., M. J. CLAUSSEN, AND L. E. TACCONI-GARMAN 1987.

OH radio observations of comet P/Halley. *Astron. Astrophys.* **187,** 469–474.

SMYTH, W. H., M. R. COMBI, AND A. I. F. STEWART 1991. Analysis of the Pioneer Venus Lyman-α image of the hydrogen coma of Comet P/Halley. *Science* **253,** 1008–1010.

STEWART, A. I. F. 1987. Pioneer Venus measurements of H, O, and C production in comet P/Halley near perihelion. *Astron. Astrophys.* **187,** 369–374.

TACCONI-GARMAN, L. E. 1989. Ph.D. thesis, University of Massachusetts.

VAN DISHOECK, E. F., AND A. DALGARNO 1984. The dissociation of OH and OD in comets by solar radiation. *Icarus* **59,** 305–313.

VAN HOOSIER, M. E., J.-D. F. BARTOE, G. E. BRUECKNER, AND D. K. PRINZ 1988. Absolute solar spectral irradiance 120nm-400nm (Results from the Solar Ultraviolet Spectral Irradiance Monitor-SUSIM-experiment on board Spacelab 2. *Astro. Lett. Commun.* **27,** 163–168.

WEAVER, H. A., P. D. FELDMAN, M. C. FESTOU, M. F. A'HEARN, AND H. U. KELLER 1981. IUE observations of faint comets. *Icarus* **47,** 449–463.

WEAVER, H. A., M. J. MUMMA, AND H. P. LARSON 1987. Infrared investigation of water in comet P/Halley. *Astron. Astrophys.* **187,** 411–418.

WEISSMAN, P. R. 1987. Post-perihelion brightening of comet P/Halley: Springtime for Halley. *Astron. Astrophys.* **187,** 873–878.

WYCKOFF, S., M. WAGNER, P. A. WEHINGER, D. G. SCHLEICHER, AND M. C. FESTOU. 1985. Onset of sublimation of comet P/Halley (1982i). *Nature* **316,** 241–242.